Int. J. Electrochem. Sci., 11 **(2016)** 10827 – 10836, doi: 10.20964/2016.12.94

International Journal of
ELECTROCHEMICAL
SCIENCE
www.electrochemsci.org

Boron Doped a-SiO_x:H Prepared by H_2 Diluted SiH_4+CO_2 Plasma

Liu Xiaojiao，Yin Junchuan，Zhang Jiawei，Li Ming，Yang Peizhi，Hu Zhihua[*]

Key Lab. of Advanced Technology & Preparation for Renewable Energy Materials, Ministry of Education, The research institute of solar energy,Yunnan Normal University, Kunming, China, 650500
[*]E-mail: 1049173841@qq.com

Received: 28 September 2016 / *Accepted:* 26 October 2016 / *Published:* 10 November 2016

This paper reports the preparation of hydrogenated amorphous silicon oxide (a-SiO_x:H) thin films by using plasma enhanced chemical vapor deposition (PECVD) technique at various doping ratios of diborane/silane(R_B=[B_2H_6]/[SiH_4]=0% 、 0.75% 、 1.5% 、 4.5% 、 7.5%), and different carbon dioxide/silane gas flow ratios (R_C=[CO_2]/[SiH_4]=0 and 1) at a substrate temperature of 200℃ (T_S = 200℃), a process pressure of 220Pa, a hydrogen dilution ratio (R_H=[H_2]/[SiH_4]=200) and a power density of 1W·cm^{-2}. We investigated the effect of various borane doping concentration on the microstrcture, optical and electrical properties of as prepared p-type a-SiO_x:H thin films via Raman spectroscopy, X-ray diffraction spectrum, ultraviolet visible light transmission spectrum (UV-VIS) and variable temperature resistance measurement method. It was found that, with the increasing of boron doping ratios, the optical band gap decreases but the refractive index increases. The dark conductivity of doped amorphous films increases monotonously with the increasing of boron doping content, while the dark conductivity of doped a-SiO_x:H films is not only determined by the concentration of dopant but also the crystallinity and oxygen content of the films. As increasing R_B, the crystallinity of doped μc-Si:H and a-SiO_x:H films simultaneously decreases, which causes the decrease of dark conductivity. Finally, B-doped a-SiO_x:H thin films with a highest dark conductivity of 0.048 Ω^{-1}·cm^{-1} have be prepared.

Keywords: Hydrogenated amorphous silicon oxide; Boron doping ratio; Dark conductivity; Activation energy.

1. INTRODUCTION

Wide optical bandgap and highly conductive p-type layers is a key for improving the photovoltaic performance. To fabricate a p-type wide bandgap layer the doping effect is usually invoked, it is an important issue to understander the influence of doping on electronic and optical

properties. However, due to the coexistence of microcrystalline and amorphous phases in the μc-Si films, the electrical and optical properties are quite complicated. The mode of dopant atoms in μc-Si such as bonding structures, sites, and electrical activities will be influnced by the microstructures. For instance, Hydrogenated silicon oxide material is a good candidate for use as the p-layer[1,2], the bandgap of the a-SiO_x:H layer could reach 1.7–2.16eV[3] depending on the oxygen content (x), and this kind of p-layer has been successfully used in the superstrate structure of glass/TCO/p-i-n/metal solar cells. In addition, several researchers have reported successful doping in nanocrystalline Si and the conductivity can be enhanced by B or P into nanocrystal doping[4-8]. This motivates further experimental investigations into nanocrystal doping. From the viewpoint of device application, further investigation of the electronic transport properties of doped nc-Si materials is necessary as various theoretical aspects and the mechanism of dopant incorporation is still under debate[9].

This report explores the microstructures, optical and electrical properties of the B-doped amorphous and microcrystallined silicon oxide thin films with various boron concentrations grown by PECVD. Through the Raman spectroscopy, X-ray diffraction spectrum, ultraviolet visible light transmission spectrum (UV-VIS) and variable temperature resistance measurement method, an attempt has been made to ascertain the growth mechainism of the highly conductive B-doped μc-SiO_x:H thin films.

2. EXPERIMENTAL

Boron doped a-SiO_x:H thin films with various boron concentrations were prepared on glass plates (76.2×25.4cm) and monocrystalline silicon substrates by using a set of multi-chamber PECVD system and a gas mixture of (SiH_4 + CO_2 + H_2 + B_2H_6) as the precursors. During the growth process, the gas flow ratios of diborane to silane (R_B = [B_2H_6]/[SiH_4]) varied from 0.75%, 0.75%, 1.5%, 4.5% to 7.5%. Carbon dioxide to silane gas flow ratios (R_C=[CO_2]/[SiH_4]) fixed as 0 and 1. Hydrogen dilution ratio (R_H = [H_2]/[SiH_4]) was kept at 200. Substrate temperature (T_S) was controlled at 200℃. The plasma was maintained with an electrode gap of 1.8cm, a power density of 1000mW·cm^{-2} and an electrode area was 240cm^2. Base pressure was 3×10^{-5}Pa. The working pressure was kept at 220Pa. The deposition conditions are shown in table 1.

The microstructures of the films were analyzied by XRD diffraction spectra and Raman scattering spectroscopy. The Optical properties of the layers were investigated by ultraviolet visible light transmission spectrum (200-2000nm) and calculation technique[10] based on Swanepeol[11] model. The temperature-dependent conductivity of samples were measured using a Fluke 1555 insulation electrometer and the activation energy was deduced from an Arrhenius plot[12, 13]. Before the dark conductivity measurements, all the samples were heated in a vacuum hermetic tube of temperature controlled, and set the temperature range as 100℃, 150℃, 200℃, 250℃ and 300℃.

Table 1. PECVD condition for deposition

R_C	R_B	R_H	Ts/°C	P.density /mW.cm^{-2}	Pressure/Pa
0 and 1	0.75 1.5 4.5 7.5	200	200	1000	220

3. RESULTS AND DISCUSSION

3.1 Research of film microstructure

Figure 4 shows the XRD diffraction spectra of p-a-Si:H and p-a-SiO_x:H thin film at R_B = 0%, 0.75%, 1.5%, 4.5% and 7.5%. In the case of p-a-Si:H material, the XRD diffraction spectra of the samples prepared at R_B = 0%, there are three obvious diffraction peaks appearing at (111), (220) and (311). With the increasing of R_B, the peaks intensity of (111) decrease distinctly, while the diffraction peaks of (220) and (311) decrease both in intensity and sharpness. The average grain size is determined by using the Debye Scherrer[14] formula as follows:

$$d_{x-ray} = \frac{k\lambda}{\beta \cos\theta} \quad (1)$$

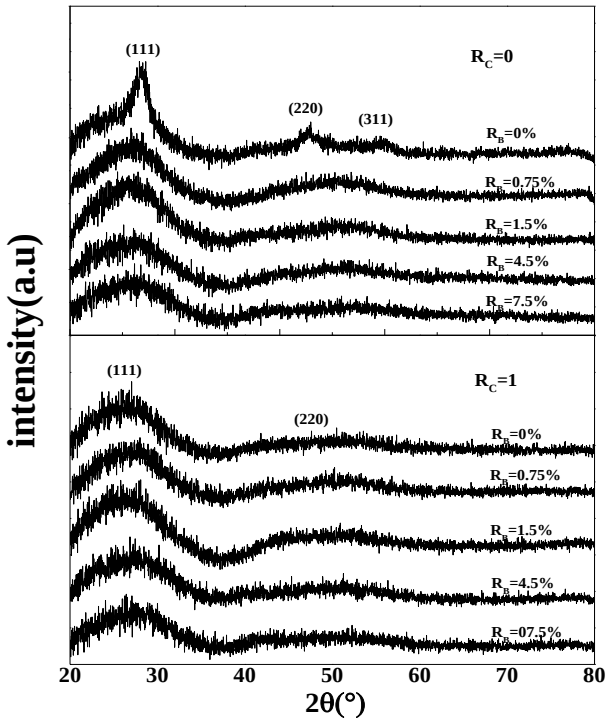

Figure 1. X-ray diffraction spectrum of thin film prepared with different doping boron ratio

Where k = 0.89, λ = 1.54056A, β denotes the full width at half maximum (FWHM) of the diffraction peak, and θ denotes the Bragg diffraction angle. From this formula, we estimated that the grain size of the p-a-Si:H thin film from the FWHM of the (220) peak. It was found that $d_{x\text{-}ray}$ decrease with the increasing of R_B from 0% to 7.5% ($d_{x\text{-}ray}$ = 2~8nm at R_B = 0%). This results imply that the

higher content of boron in the Si network gives rise to amorphization in the μc-Si film structure. This is mainly associated with the doping effect of boron and the atomic hydrogen etching effect[15,16]. Furthermore, it can be seen from Fig.1 that the three peaks of p-a-SiO_x:H thin films are not appeared with the increasing of R_B. The changes of the preferential crystallographic growth direction may be ascribed to the doping with carbon dioxide. In spite of this, XRD spectra results give the same trend of the evolution of the crystalline phase as that of Raman spectra when the R_B is increased.

For comparison, the Raman spectra of p-a-Si:H and p-a-SiO_x:H thin films prepared with the different R_B are shown in Fig. 2. The signals at 480cm^{-1} and 520cm^{-1} represent the transverse-optical (TO) vibration mode of amorphous silicon and the (TO) vibration mode of the crystalline silicon, respectively.

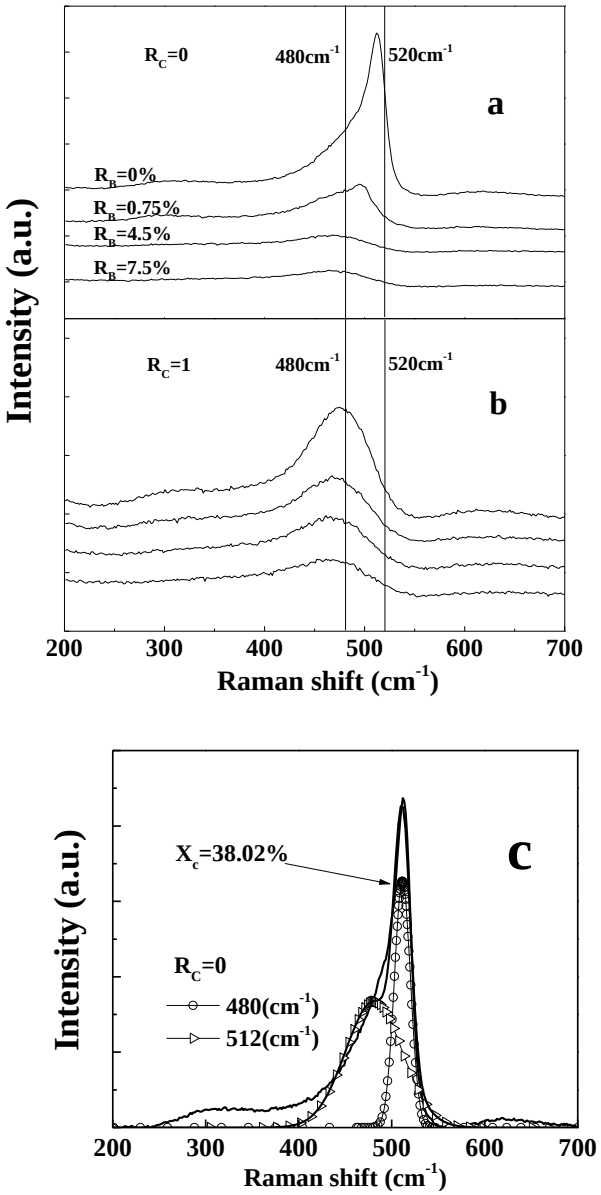

Figure 2. Raman spectra of films prepared with different B_2H_6/SiH_4 doping ratios

As shown in Fig. 2 (a), there is an observable protrusion appearing at about 512cm^{-1} at the R_B = 0%, which is the corresponding crystalline phase, is obviously detected. When the doping ratio R_B increase from 0% to 7.5%, there are no observable crystalline peaks, indicating that the films completely entered the amorphous phase. However, for samples doping with carbon dioxide, the broad band peaks appear at around 480cm^{-1}, as shown in Fig.2 (b), which indicate that as-deposited samples exhibit purely amorphous structures. The results show that when the R_B are increased and the CO_2 are added, the μc-Si:H phase tend to decrease while the a-Si:H phase trend to increase. The crystalline volume fraction (X_c) shown in Fig. 2 (c) was deduced from Raman spectral results by the formula[17]:

$$X_C = \frac{I_c + I_b}{0.9 \times I_a + I_b + I_c} \times 100 \quad (2)$$

Where I_a denotes the integrated area corresponding to amorphous phases in 470~480 cm^{-1}, I_b denotes the integrated area corresponding to intermediate phases 506~512 cm^{-1}, I_c denotes the integrated area corresponding to crystalline phases in 519~522 cm^{-1}, and 0.9 denotes the correction coefficient. We found that X_c gradually decrease from 38.02% to 27.5% with the increasing of R_B from 0% to 0.75%. The observations give the same trend of the reported by R. Saleh et al., and it has been suggested that this effect is due to an increase in bond-angle and bond-length fluctuations as the dopant atom incorporated in the film causing the degradation of the short-range order[18]. Therefore, the reduction of crystallinity with the increase of R_B should be caused by the increase of dopant concentration. Meanwhile, according to N. H. Nickel et al., as increasing the concentration of boron, the Raman spectra will be distorted and become weak due to the Fano effect[19]. As a result, the decrease of intensity of the Raman spectra with the increase of R_B should be caused by the increase of amorphous component and the Fano effect in the doped microcrystalline films.

3.2 Optical and electrical properties

Figure 4 shows the transmission spectra of p-a-Si:H and p-a-SiO_x:H thin films prepared with different boron doping ratios. It can be seen that the transmittance decrease sharply in the short wave period of p-a-Si:H film with the increasing of R_B, which are shifted toward higher photon energy. For samples doped with CO_2, the transmittance are higher monotonously in comparison with the conventional p-a-Si:H film counterpart. This is because of the increased number of Si-O bonds in the SiO_x:H films[20,21].

A Tauc plot was usually used to describe the light absorption of an amorphous semiconductor Si films. In the present work, we have found for our samples a fairly good linearity of the $(\alpha h\nu)^{1/2}$ versus hv plot as shown in Fig. 5. This is the Tauc equation:

$$\sqrt{\alpha h\nu} = A_0\left(h\nu - E_g\right) \quad (3)$$

is widely used to define the band gap of amorphous semiconductors characterizing the transitions between the extended states.

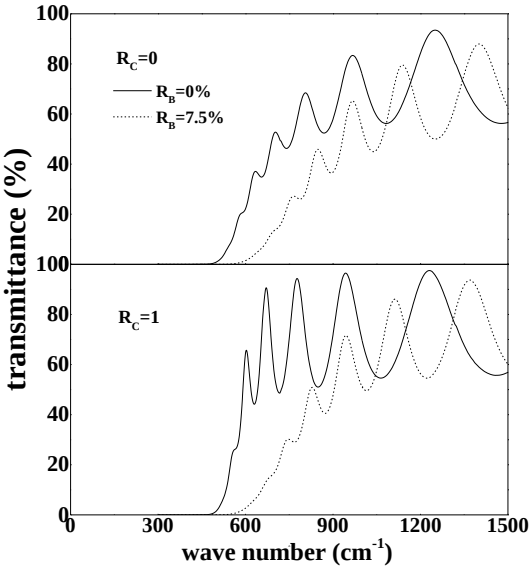

Figure 4. Transmission spectra of thin films prepared with different boron doping ratios

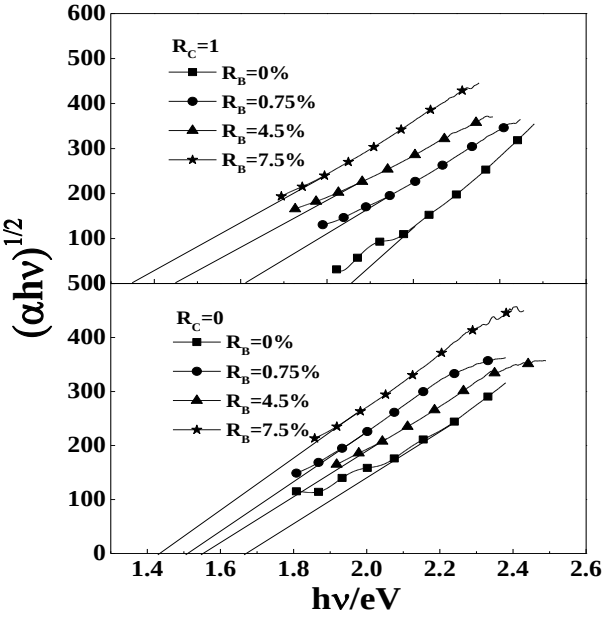

Figure 5. Tauc's plot of thin films prepared with different boron doping ratios

It can be seen that the optical band gap decreases monotonously with the increasing of R_B. For the as-deposited p-a-Si:H films grown, the optical band gaps are varied from 1.68eV to 1.43eV and are enlarged to 2.04eV after doping with CO_2 (R_C = 1) that due to the increased number of Si-O bonds in the p-a-SiO_x:H films. This results are similar to the observation of the transmission spectra. Extrapolating photon energy-dependent refractive indices to the non-absorbing region (extinction coefficient → 0), their estimated values n in the long wavelength limit[22] are shown in Fig. 6. The refractive index is an important wavelength-independent optical parameter related to the atomic structure and the mass density.

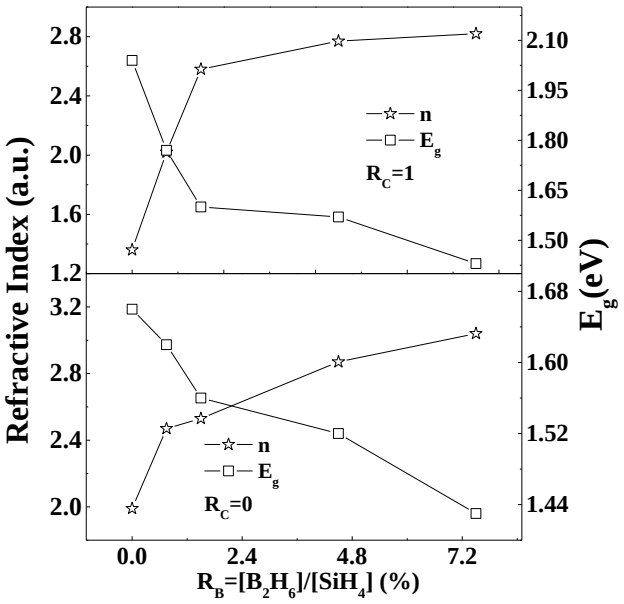

Figure 6. Refractive index and optical band gap variation of thin films prepared with different CO_2/SiH_4 gas flow ratios

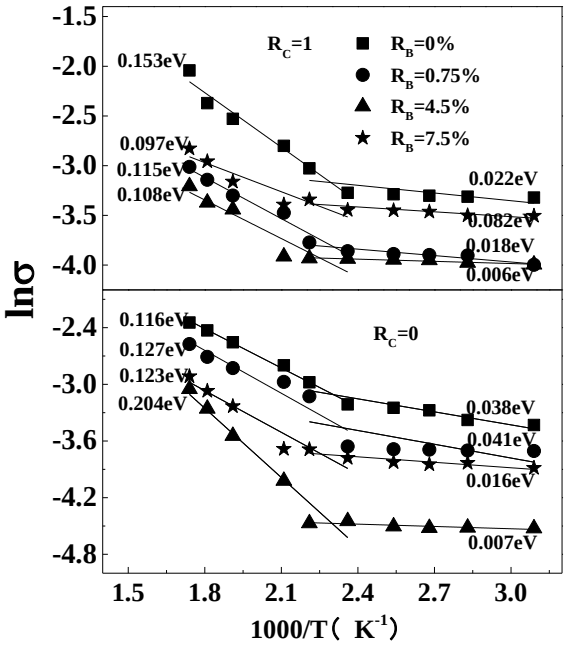

Figure 7. Dark conductivity σ_d and temperature T variation of thin films prepared with different doping boron ratios

We can see that there are the increase in the refractive index with the increasing of R_B that can be attributed to the increase of the films mass density. While the refractive index of the p-SiO_x:H film grown using carbon dioxide is lower than that of the film without any carbon dioxide, the oxygen-rich amorphous phase leads to a low refractive index and high band gap[23].

Figure 7 gives the temperature-dependent conductivity for the as-deposited samples grown at different $R_{B,}$ the conductivity activation energy E_a is obtained using the slope of lnσ versus T^{-1} curve. The results were described according to Arrhenius plots:

$$\sigma_d(T) = \sigma_0 \exp(\frac{-E_a}{k_B \cdot T}) \quad (4)$$

Where σ_0 denotes the conductivity prefactor, T denotes the absolute temperature, k_B denotes the Boltzmann's constant, and E_a is the conductivity activation energy.

The value of σ_d and E_a as a function of R_B is shown in Figure 8. With the increasing of R_B from 0% to 7.5%, it can be found that the temperature dark conductivity of the p-a-Si:H films are decreased from 0.06 $\Omega^{-1}\cdot cm^{-1}$ to 0.029$\Omega^{-1}\cdot cm^{-1}$. According to the results of the Raman and XRD spectra, the decreasing of dark conductivity is mainly attributed to the decreasing of crystallinity even though the carrier concentration increases as the increasing of R_B. Meanwhile, the corresponding values of conductivity activation energy increase from 0.115eV to 0.32eV. However, when R_B = 1.5%, a break in the dark conductivity and activation energy appears; this transition of doped a-Si:H films should be caused by the increasing of doping content. Comparing with the B-doped a-Si:H films, the electrical properties of p-a-SiO_x:H films seem to become poorer, the dark conductivity decrease from 0.042$\Omega^{-1}\cdot cm^{-1}$ to 0.023$\Omega^{-1}\cdot cm^{-1}$, while the corresponding value of the conductivity activation energy increase from 0.116eV to 0.308eV with the R_B between 0% and 1.5%.

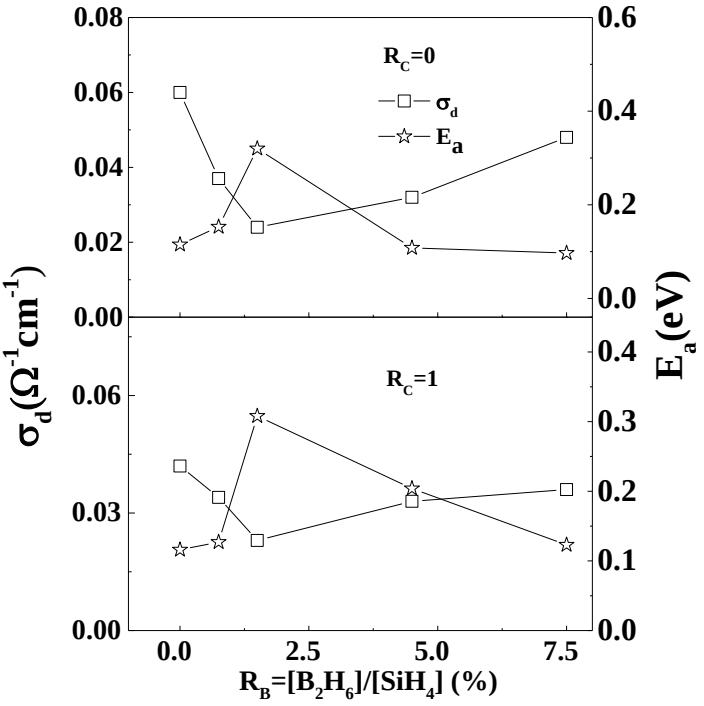

Figure 8. dark conductivity σ_d and activation energy E_a variation of thin films prepared with different doping boron ratios

This results are mainly due to the increased number of Si-O bonds in the SiO_x:H films[20,21], its being the same as the thransmittance spectra. While the increasing of R_B from 1.5% to 7.5%, the dark conductivity increase significantly from 0.023$\Omega^{-1}\cdot cm^{-1}$ to 0.036$\Omega^{-1}\cdot cm^{-1}$, and the conductivity

activation energy decrease from 0.308eV to 0.123eV. As a result, the increase in dark conductivity and the decrease in the corresponding activation energy of the B-doped a-SiO_x:H samples are caused by the increase of the doping content[24]. Therefore, for the B-doped a-Si:H samples, the decrease of dark conductivity is mainly due to boron doping amorphization effect leading to the decrease of crystallinity as increasing R_B. While it is also noted that the B-doped μc-Si phase contributes to achieving a sufficient dark conductivity[25].

4. CONCLUSION

The B_2H_6/SiH_4 ratio for the p-a-SiO_x:H film plays a key role in controlling the structural, electrical, and optical properties of films. By using XRD spectra, it was found that the samples (R_C = 1) deposited with different R_B are amorphous with no presence of the crystalline phase, but the sample deposited at R_C = 0 and R_B = 0% appeares in obviously diffraction peaks. Raman measurement analysis substantiated the results received from XRD, showing that the microcrystalline phase transfers to amorphous phase with the increasing of R_B, and the crystallized fraction X_c of a-Si:H film decreases from 38.02% to 27.5%. The optical characterization based on transmittance spectra in the visible region show that the refractive index exhibits an upward trend with the increasing of R_B, which can be caused by the densification of the amorphous network. Moreover, we discovered that the optical band gap decreases monotonously with the increasing of R_B, and it is enlarged from 1.68eV to 2.04eV after doping with CO_2 (R_C = 1) that mainly due to the increased number of Si-O bonds in the p-a-SiO_x:H films. According to the temperature-dependent conductivity measurements, it was found that the boron dopant causes the conductivity to increase and the activation energy to decrease with the increasing of R_B due to the greater dopant content as R_B increased.

ACKNOWLEDGEMENT
This work was supported by the Collaborative Innovation Center of Development of Renewable Energy in the Southwest Area Programmer NO. 05300205020516009.

References

1. Y. Hattori, D. Kruangam, T. Toyama, H. Okamoto, Y. Hamakawa, *J. Non-Crystalline Solids.*, 1079 (1987) 97-98.
2. S. Fujikake, H. Ohta, P. Sichanugrist, M. Ohsawa, Y. Ichikawa, H. Sakai, Optoelectronics-Devices Technologies 3 (1994) 379-90.
3. K. Sriprapha, C. Piromjit, A. Limmanee, N. Sitthipol, S. Kittisontirak, A. Moollakorn,V. Sangsuwan, P. Sichanugrist, Proceedings of MRS Spring Meeting, SanFrancisco, 2009, A7.6.
4. K. Sato, N. Fukata, K. Hirakuri, *J. Appl. Phys. Lett.*, 94 (2009) 161902.
5. A. R. Stegner, R. N. Pereira, K. Klein, R. Lechner, R. Dietmueller, M. S. Brandt, M. Stutzmann, H. Wiggers, *J. Phys. Rev. Lett.*, 100 (2008) 161902.
6. X. J. Hao, E. C. Cho, C. Flynn, Y. S. Shen, S. C. Park, G. Conibeer, M. A. Green, *J. Sol. Energy Mater Sol. Cells.*, 93 (2009) 273-279.
7. C.-S. Jiang, B. Yan, Y. Yan, C.W. Teplin, R. Reedy, H. R. Moutinho, M. M. Al-Jas-sim, J. Yang,

J. Appl. Phys., 103 (2008) 063515.
8. C.-S. Jiang, B. Yan, Y. Yan, C.W. Teplin, R. Reedy, H. R. Moutinho, M.M. Al-Jas-sim, J. Yang, S. Guha, *J. Non-CRYST. Soilds.*, 354 (2008) 2276-2281.
9. J. D. Norris, L. A. Efros, C. S. Erwin, *J. Science.*, 319 (2008) 1176-1779.
10. Zhihua Hu and Xianbo Liao, *J. Journal of Semiconductors.*, 26 (2005) 34-37.
11. Swanepoel R, *J. Phys E.*, 16 (1983) 1214-1222.
12. Yuliang He, Guanghua Chen, Fangqing Zhang, *M. publishing house of higher education.*, 1989.
13. Enke Liu, Bingsheng Zhu, *M. publishing house of Xi'an Jiaotong University.*, 1998.
14. S. Jia, H. Ge, X. Geng, *J. Solar Energy Materials and Solar Cetts.*, 62 (2000) 201-205.
15. H. Chen, M. H. Gullanara, W. Z. Shen, *J. Cryst. Growth.*, 260 (2004) 91–101.
16. V. S. Waman, M. M. Kamble, S. S. Ghosh, A. H. Mayabadi, B. B. Gabhale, S. R. Rondiya, A.V. Rokade, S. S. Khadtare, V. G. Sathe, H.M. Pathan, S.W. Gosavi, S. R. Jadkar, *J. Alloys Compd.*, 585 (2014) 523–528.
17. D. Das, M. Jana, and A. K. Barua, *J. Solar Energy Materials and Solar Cells.*, 63 (2000) 285-297.
18. R. Saleh, N.H. Nickel, Appl. Surf. Sci. 254 (2007) 580e585.
19. N.H. Nickel, P. Lengsfeld, I. Sieber, Phys. Rev. B. 61 (2000) 15558e15561.
20. S. Miyajima, A. Yamada, and M. Konagai, *J. Thin Solid Films.*, 430 (2003), 274–277.
21. T. Krajangsang, S. Kasashima, A. Hongsingthong, P. Sichanu-grist, and M. Konagai, *J. Current Applied Physics.*, 12 (2012), 515-520.
22. S. Arvind, J. Meier, E. V. Sauvain, *J. Thin solid films.*, 2002: 403-404, 179-187.
23. Buehlmann, P. Bailat, J. Domine, D. Billet, A. Meillaud, F. Feltrin, A. Ballif, C., *J. Appl. Phys. Lett.*, 91 (2007), 143505.
24. K. Shimakawa, *J. Non-Cryst. Solids.*,266-269 (2000), 223-226.
25. Grundler, T., Lambertz, A., Finger, F., *J. Phys. Status. Solidi.*, C7 (2010) 1085.